

Addition of CO₂ to Alkyl Iron Complexes, Fe(PP)₂Me₂

Olivia R. Allen,[†] Scott J. Dalgarno,^{▲,△} Leslie D. Field,^{*,†} Paul Jensen,[‡]
Anthony J. Turnbull,[†] and Anthony C. Willis[§]

School of Chemistry, The University of New South Wales, NSW 2052, Australia, School of Chemistry, University of Sydney, NSW 2006, Australia, Department of Chemistry, Australian National University, Canberra, ACT 0200, Australia, Department of Chemistry, University of Missouri–Columbia, Columbia, Missouri 65211, and School of EPS–Chemistry, Heriot-Watt University, Riccarton, Edinburgh, EH14 4AS, U.K.

Received January 31, 2008

The reactions of *cis*- and *trans*-Fe(dmpe)₂Me₂ (**1**) [dmpe = 1,2-bis(dimethylphosphino)ethane] and *cis/trans*-Fe(depe)₂Me₂ (**6**) [depe = 1,2-bis(diethylphosphino)ethane] with carbon dioxide (CO₂) were investigated along with the isomerization properties of the starting materials **1** and **6**. Irradiation with UV light cleanly isomerizes the dimethyl complexes from their *cis* configurations **1a** and **6a** to their *trans* configurations **1b** and **6b**. At 300 K, addition of CO₂ (1 atm) to **1** or **6** forms a stable methyl acetate, Fe(dmpe)₂(OCOCH₃)Me (**2**) or Fe(depe)₂(OCOCH₃)Me (**7**), respectively, by insertion of CO₂ into one of the metal–carbon bonds. At 330 K, the addition of CO₂ (5–6 atm) to **1** results in the initial formation of the methyl acetate (**2**) followed by the formation of an octahedral bis-acetate complex Fe(dmpe)₂(OCOCH₃)₂ (**3**), which was also synthesized independently. Complex **3** rearranges to a salt containing a bidentate acetate and an acetate counterion, [Fe(dmpe)₂(OCOCH₃)₂]⁺[OCOCH₃][−] (**4**). The depe analogue to **3**, Fe(depe)₂(OCOCH₃)₂ (**8**), was not observed in the reaction between **6** and CO₂, and only the salt [Fe(depe)₂(OCOCH₃)₂]⁺[OCOCH₃][−] (**9**) was isolated. In the reactions of either *cis*- or *trans*-Fe(dmpe)₂Me₂ (**1**) with CO₂, a stable carbonate complex, Fe(dmpe)₂(CO₃) (**5**), with a bidentate carbonate ligand, was also observed. All complexes were characterized by multinuclear NMR spectroscopy, with IR spectroscopy and elemental analyses confirming structures of thermally stable complexes where possible. Complexes **1b**, **3**, **5**, **6b**, and **9** were characterized by X-ray crystallography.

Introduction

The development of practical methods for carbon dioxide fixation is essential in the management of this greenhouse gas, and this has been the subject of much discussion and research in recent times.¹ Carbon dioxide has great potential as an inexpensive and abundant source of carbon for use in organic synthesis.^{2–6} An important step in the functionalization of small

molecules such as carbon dioxide is their insertion into reactive metal–hydride and metal–carbon bonds.^{7–10}

Previously, we have reported the insertion of CO₂ into the metal–hydride bonds of *cis*-Fe(dmpe)₂H₂ (dmpe = Me₂PCH₂–CH₂PMe₂) and *cis*-Fe(PP)₃H₂ (PP₃ = P(CH₂CH₂PMe₂)₃),¹¹ and the insertion products include the expected metal formates Fe(dmpe)₂(OCHO)H and Fe(PP₃)(OCHO)H. When an excess of CO₂ was used in these reactions, the bis-insertion products were observed although the second insertion is reversible and, on removal of the CO₂ atmosphere, the bis-formates decarboxylate and revert to the hydrido formate complexes. Perutz et al.^{12–14} and Baiker et al.^{12–14} have reported similar products from the reaction of the ruthenium analogue *cis*-Ru(dmpe)₂H₂ with CO₂, and the monoinsertion product Ru(PMe₃)₄(OCHO)H from the reaction of Ru(PMe₃)₄H₂ and CO₂ has also been reported.⁸

* To whom correspondence should be addressed. Fax: +61 2 9385 2700. Tel: +61 2 9385 8008. E-mail: L.Field@unsw.edu.au.

[†] The University of New South Wales.

[‡] University of Sydney.

[§] Australian National University.

[▲] University of Missouri–Columbia.

[△] Heriot-Watt University.

(1) Arakawa, H.; Aresta, M.; Armor, J. N.; Barteau, M. A.; Beckman, E. J.; Bell, A. T.; Bercaw, J. E.; Creutz, C.; Dinjus, E.; Dixon, D. A.; Domen, K.; DuBois, D. L.; Eckert, J.; Fujita, E.; Gibson, D. H.; Goddard, W. A.; Goodman, D. W.; Keller, J.; Kubas, G. J.; Kung, H. H.; Lyons, J. E.; Manzer, L. E.; Marks, T. J.; Morokuma, K.; Nicholas, K. M.; Periana, R.; Que, L.; Rostrup-Nielsen, J.; Sachtler, W. M. H.; Schmidt, L. D.; Sen, A.; Somorjai, G. A.; Stair, P. C.; Stults, B. R.; Tumas, W. *Chem. Rev.* **2001**, *101*, 953–996.

(2) Gibson, D. H. *Chem. Rev.* **1996**, *96*, 2063–2095.

(3) Gibson, D. H.; Sleadd, B. A.; Ding, Y.; Mehta, J. M.; Franco, J. O.; Richardson, J. F.; Mashuta, M. S. *Book of Abstracts, 215th ACS National Meeting, Dallas, March 29–April 2 1998*, COLL-082.

(4) Leitner, W. *Coord. Chem. Rev.* **1996**, *153*, 257–284.

(5) Dinjus, E.; Leitner, W. Transition metal catalyzed activation of carbon dioxide. In *Carbon Dioxide Chemistry: Environmental Issues*; Paul, J., Pradier, C.-M., Eds.; Royal Society of Chemistry: Cambridge, 1994; Vol. 153, pp 82–92.

(6) Aresta, M. Carbon dioxide reduction and uses as a chemical feedstock. In *Activation of Small Molecules*; Tolman, W. B., Ed.; Wiley-VCH: Weinheim, 2006; pp 1–42.

(7) Aresta, M.; Quaranta, E.; Tommasi, I. *New J. Chem.* **1994**, *18*, 133–142.

(8) Jessop, P. G.; Hsiao, Y.; Ikariya, T.; Noyori, R. *J. Am. Chem. Soc.* **1996**, *118*, 344–355.

(9) Yin, X.; Moss, J. R. *Coord. Chem. Rev.* **1999**, *181*, 27–59.

(10) Behr, A. Insertion Reactions of Carbon Dioxide. CO₂ Insertion into the M–C Bond. In *Carbon Dioxide Activation by Metal Complexes*; VCH: Weinheim, 1988; pp 31–45.

(11) Field, L. D.; Lawrenz, E. T.; Shaw, W. J.; Turner, P. *Inorg. Chem.* **2000**, *39*, 5632–5638.

(12) Whittlesey, M. K.; Perutz, R. N.; Moore, M. H. *Organometallics* **1996**, *15*, 5166–5169.

(13) Urakawa, A.; Jutz, F.; Laurenczy, G.; Baiker, A. *Chem.–Eur. J.* **2007**, *13*, 3886–3899.

(14) Baiker, A.; Urakawa, A.; Iannuzzi, M.; Hutter, J. *Chem.–Eur. J.* **2007**, *13*, 6828–6840.

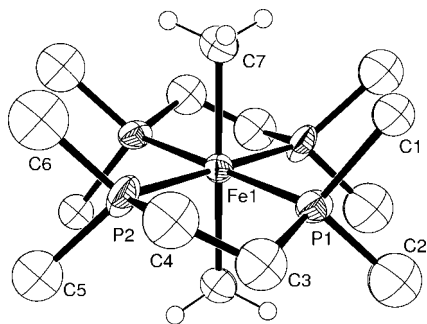


Figure 1. ORTEP diagram of *trans*-Fe(dmpe)₂Me₂ (**1b**) (50% ellipsoids and only one component of each of the disordered atoms is shown). Selected hydrogen atoms have been omitted for clarity.

Examples of CO₂ activation by iron phosphine complexes are relatively rare,^{15–19} and in this paper, we report the insertion of carbon dioxide into the iron(II)–carbon bonds of *cis*- and *trans*-Fe(dmpe)₂Me₂ (**1**) and *cis*- and *trans*-Fe(depe)₂Me₂ (**6**). CO₂ insertion into an iron–carbon bond has been reported previously by Tolman et al.,²⁰ who reported the insertion of CO₂ into the Fe–C bond of FeH(dmpe)₂(CH₂CN) to eventually form cyanoacetic acid.

Results and Discussion

The dimethyliron(II) complex Fe(dmpe)₂Me₂ (**1**) was synthesized in an analogous manner to that reported by Wilkinson et al.²¹ by alkylating Fe(dmpe)₂Cl₂ using methylolithium as the alkylating agent. The related complex Fe(depe)₂Me₂ (**6**) was prepared from Fe(depe)₂Cl₂.²² In solution, both dimethyl complexes exist as mixtures of *cis*-isomers (**1a** and **6a**) and *trans*-isomers (**1b** and **6b**). Crystals of the *trans*-isomers of both dimethyl complexes, suitable for analysis by X-ray crystallography, were grown by low-temperature (265 K) crystallization from pentane. ORTEP diagrams of *trans*-Fe(dmpe)₂Me₂ (**1b**) and *trans*-Fe(depe)₂Me₂ (**6b**) are given in Figures 1 and 2, and selected bond lengths and angles are listed in Tables 1 and 2, respectively.

The X-ray crystal structures of both **1b** and **6b** show a classic octahedral arrangement of the ligands around the metal with inversion symmetry on the metal sites in both structures. Unlike **1b**, which has a single unique “half complex” (with a disordered dmpe ligand), **6b** contains two crystallographically unique “half complexes” in the asymmetric unit. (One of these has a disordered depe ligand and is omitted from Figure 2). The bond lengths and bond angles in the crystal structures of **1b** and **6b**

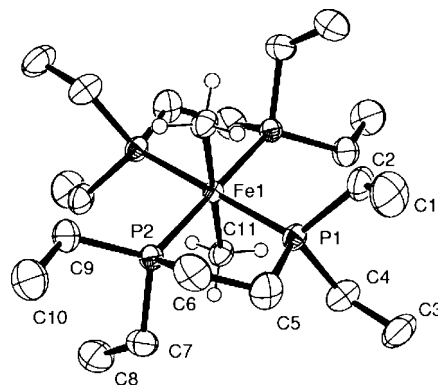


Figure 2. ORTEP diagram of *trans*-Fe(depe)₂Me₂ (**6b**) (50% ellipsoids; only one component of the two crystallographically unique complexes is shown). Selected hydrogen atoms have been omitted for clarity.

Table 1. Selected Bond Distances and Angles for *trans*-Fe(dmpe)₂Me₂ (**1b**)

Bond Distances (Å)			
Fe(1)–P(1)	2.169(13)	Fe(1)–P(2)	2.180(8)
Fe(1)–C(7)	2.128(4)		
Bond Angles (deg)			
C(7)–Fe(1)–C(7)	180.000(10)	P(1)–Fe(1)–P(2)	88.0(3)
P(2)–Fe(1)–C(7)	90.4(3)	P(1)–Fe(1)–C(7)	94.1(3)

Table 2. Selected Bond Distances and Angles for *trans*-Fe(depe)₂Me₂ (**6b**)

Bond Distances (Å)			
Fe(1)–P(1)	2.2049(11)	Fe(1)–P(2)	2.2092(11)
Fe(1)–C(11)	2.124(11)		
Bond Angles (deg)			
C(11)–Fe(1)–C(11)	180.00(1)	P(1)–Fe(1)–P(2)	84.63(4)
P(2)–Fe(1)–C(11)	93.71(13)	P(1)–Fe(1)–C(11)	91.93(12)

are unexceptional and are comparable with other iron phosphine dimethyl complexes reported in the literature.^{23,24}

Cis- and Trans-Isomers of Fe(dmpe)₂Me₂ (1**) and Fe(depe)₂Me₂ (**6**).** Both complexes **1** and **6** exist as equilibrating mixtures of *cis*- and *trans*-isomers in solution. In Wilkinson’s original synthesis of *cis*-Fe(dmpe)₂Me₂ (from *trans*-Fe(dmpe)₂Cl₂ using Me₂Mg as the alkylating agent at room temperature), it was noted that the synthesis must be completed and the product worked up in a short time to avoid partial isomerization to the *trans* product.²¹

When benzene solutions of *cis*- and *trans*-**1** or *cis*- and *trans*-**6** were irradiated using a high-pressure mercury vapor lamp, the complexes isomerized quantitatively to the *trans*-isomers with the reactions complete within 30 min. When a solution of *trans*-Fe(depe)₂Me₂ (**6b**) was left to stand at room temperature, the complex partially isomerized back to the *cis* species and equilibrium was attained over the space of about 2.5 h with the resulting mixture containing approximately 18% *trans*- and 82% *cis*-isomers. Kinetic analysis of the thermal isomerization of **6b** to **6a** gives a Δ*G*[‡] of 92.0 kJ mol^{–1} at 295 K. The fact that the photoisomerization reaction produces exclusively the *trans*-isomers of **1** and **6** suggests that light absorption, which promotes isomerization of the complexes, is more favorable in the *cis*-isomers than in the *trans*-isomer, and this effectively “pumps” the *cis*-isomer to the *trans* stereochemistry. The mixture of isomers at equilibrium is temperature dependent, with the *cis*-isomer being the dominant species at lower temperatures (**6a**:**6b** = 82:18 at 295 K; **6a**:**6b** = 54:46 at 335 K).

(15) Hirano, M.; Akita, M.; Tani, K.; Kumagai, K.; Kasuga, N. C.; Fukuoka, A.; Komiya, S. *Organometallics* **1997**, *16*, 4206–4213.

(16) Komiya, S.; Akita, M.; Kasuga, N.; Hirano, M.; Fukuoka, A. *J. Chem. Soc., Chem. Commun.* **1994**, 1115–1116.

(17) Lu, C. C.; Saouma, C. T.; Day, M. W.; Peters, J. C. *J. Am. Chem. Soc.* **2007**, *129*, 4–5.

(18) Karsch, H. H. *Chem. Ber.* **1977**, *110*, 2213–2221.

(19) Hoberg, H.; Jenni, K.; Angermund, K.; Kruger, C. *Angew. Chem., Int. Ed.* **1987**, *26*, 153–155.

(20) Ittel, S. D.; Tolman, C. A.; English, A. D.; Jesson, J. P. *J. Am. Chem. Soc.* **1978**, *100*, 7577–7585.

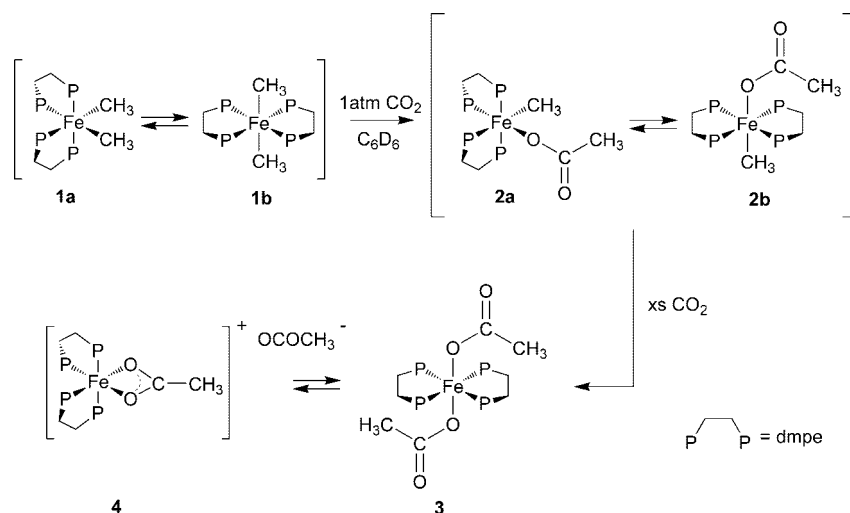
(21) Girolami, G. S.; Wilkinson, G.; Galas, A. M. R.; Thornton-Pett, M.; Hursthouse, M. B. *Dalton Trans.* **1985**, 1339–1348.

(22) Karsch, H. H. *Chem. Ber.* **1977**, *110*, 2712–2720.

(23) Fang, X.; Scott, B. L.; Watkin, J. G.; Kubas, G. J. *Organometallics* **2001**, *20*, 2413–2416.

(24) Venturi, C.; Bellachioma, G.; Cardaci, G.; Macchioni, A.; Zuccaccia, C. *Inorg. Chim. Acta* **2005**, *358*, 3815–3823.

Scheme 1



The stereochemistry of *trans*-Fe(dmpe)₂Me₂ (**1b**) is significantly more stable in solution; however the complex isomerized slowly on heating in toluene at 95 °C. After about 20 h, an equilibrium mixture is obtained, and this contains approximately 73% *cis*- and 27% *trans*-isomers. Kinetic analysis of the thermal isomerization of **1b** to **1a** gives a ΔG^\ddagger of 121.2 kJ mol⁻¹ at 368 K.

The dimethyliron (II) complexes are clearly stereochemically labile. A probable mechanism of isomerization would be via phosphine dissociation.^{25–28} The faster rate of thermal isomerization of **6** compared to **1** can be attributed to the weaker binding of the bulkier depe ligand, compared to that of the dmpe ligand, resulting in more facile phosphine dissociation.

Carbon Dioxide Insertion into Fe–CH₃ Bonds. Solutions of Fe(dmpe)₂Me₂ (**1**) in tetrahydrofuran-*d*₈ and benzene-*d*₆ react with ¹³CO₂ (at 1 atm and 300 K) to form the monoinsertion product *trans*-Fe(dmpe)₂(O₂CCH₃)Me (**2b**). This product gives rise to a singlet resonance at 71.1 ppm in the ³¹P{¹H} NMR spectrum after 1 h at 300 K in C₆D₆. There is also a distinctive pentet in the ¹H spectrum at –3.29 ppm, characteristic of the metal-bound methyl group which is coupled to the four equivalent phosphorus atoms. The methyl resonance is shifted approximately 1.34 ppm to high field of the corresponding pentet for the *trans*-dimethyl complex (**1b**). By employing ¹³C-labeled carbon dioxide in the synthesis, the acetate quaternary carbon can be clearly observed in the ¹³C{¹H} spectrum at 176.2 ppm. This complex has been reported previously,²⁰ and an authentic sample was also prepared independently, during the course of this work, by the reaction of **1** with 1 equiv of acetic acid in diethyl ether. *cis*-Fe(dmpe)₂(O₂CCH₃)Me (**2a**) is also briefly observed in the reaction with CO₂ but only as a transient species. The *trans*-isomer is configurationally stable at room temperature; however irradiation with UV light at room temperature leads to a mixture of the *cis* and *trans* complexes in the ratio of approximately 58% to 42%, respectively. When this mixture is warmed to 343 K, **2a** immediately isomerizes to **2b**, indicating that the energy barrier between the two isomers is small. The ³¹P{¹H} NMR spectrum of the *cis*-isomer shows four sets of

signals attributable to the four chemically inequivalent phosphorus atoms. There is a large P–P coupling (166.9 Hz) between the phosphorus atoms *trans* to each other.

If higher pressures of CO₂ (up to 6 atm) and higher temperatures (up to 333 K) are used, then the reaction proceeds more quickly, and after 15 min the initial monoinsertion product can be detected and after about two days a doubly inserted *trans*-diacetate complex (**3**) can be detected (Scheme 1). Under these reaction conditions, the reaction does not proceed to completion and insertion into the second Fe–C bond of **1** is significantly slower than insertion into the first.

Complex **3** has been synthesized independently by the reaction of iron(II) acetate with 2 equiv of dmpe in THF to give a blue crystalline solid, which has been characterized by NMR spectroscopy, FTIR spectroscopy, and X-ray crystallography. The ³¹P{¹H} NMR confirms the existence of one *trans* species with a singlet at δ 64.4 ppm, and the ¹H NMR spectrum shows a broadened singlet at 1.22 ppm, which can be attributed to the protons of the acetate groups. The ¹³C{¹H} NMR spectrum has a resonance at 177.3 ppm for the carbonyl carbon. The FTIR spectrum for this complex shows a ν_{asym} at 1605 cm⁻¹, which is similar to that observed for other complexes of this type.²⁰ The *trans*-isomer is configurationally stable, and even under irradiation with UV light, the *cis*-isomer is not formed.

Blue crystals of **3** suitable for a structure determination were grown from a solution of DMF and pentane (Figure 3). The asymmetric unit of **3** contains half of one complex with 2-fold symmetry generating the other half. The iron(II)–acetate (Fe–O) bond length (2.0132 Å) is slightly shorter than that in the analogous formate complex Fe(dmpe)₂(OCHO)₂ (2.018 Å)¹¹ (Table 3).

trans-Fe(dmpe)₂(CO₂CH₃)₂ (**3**) is relatively insoluble in nonpolar solvents; however when dissolved in more polar solvents such as methanol or DMF, the solutions are red in color. The ³¹P{¹H} NMR spectrum of the red product displays two apparent triplets characteristic of symmetrically substituted Fe(dmpe)₂X₂ complexes with the X substituents arranged in a *cis* geometry. This behavior is the result of rearrangement of the complex with one of the acetate ligands adopting a bidentate η^2 -binding mode to form a cationic complex with the loss of one acetate. The reaction is low yielding with respect to **3**, and there is probably an equilibrium in solution between the different acetate binding modes in **3** and **4** (Scheme 1).

(25) Bianchini, C.; Meli, A.; Peruzzini, M.; Frediani, P.; Bohanna, C.; Esteruelas, M. A.; Oro, L. A. *Organometallics* **1992**, *11*, 138–145.

(26) Bianchini, C.; Masi, D.; Meli, A.; Peruzzini, M.; Zanobini, F. *J. Am. Chem. Soc.* **1988**, *110*, 6411–6423.

(27) Thaler, E. G.; Foltling, K.; Caulton, K. G. *J. Am. Chem. Soc.* **1990**, *112*, 2664–2672.

(28) Thaler, E. G.; Caulton, K. G. *Organometallics* **1990**, *9*, 1871–1876.

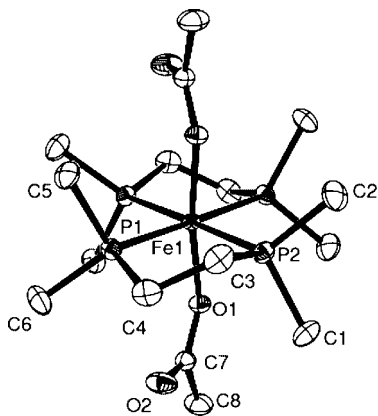


Figure 3. ORTEP diagram of *trans*-Fe(dmpe)₂(O₂CCH₃)₂ (**3**) (50% ellipsoids with hydrogen atoms omitted for clarity).

Table 3. Selected Bond Distances and Angles for *trans*-Fe(dmpe)₂(O₂CCH₃)₂ (**3**)

Bond Distances (Å)			
Fe(1)–P(1)	2.2385(3)	Fe(1)–P(2)	2.2485(3)
Fe(1)–O(1)	2.0132(8)	O(1)–C(7)	1.2756(14)
O(2)–C(7)	1.2369(14)	C(7)–C(8)	1.5184(16)
Bond Angles (deg)			
O(1)–Fe(1)–O(1)	172.27(5)	P(1)–Fe(1)–P(2)	85.207(14)
P(1)–Fe(1)–O(1)	93.31(2)	P(2)–Fe(1)–O(1)	99.72(2)
O(1)–C(7)–O(2)	126.59(11)	O(2)–C(7)–C(8)	119.35(11)
O(1)–C(7)–C(8)	114.06(10)		

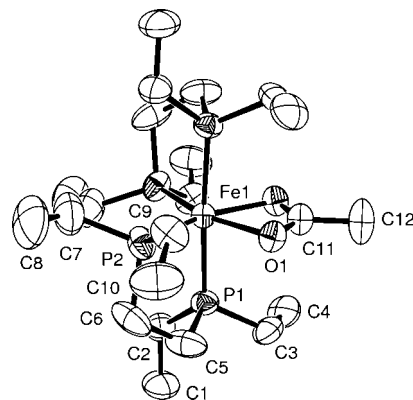
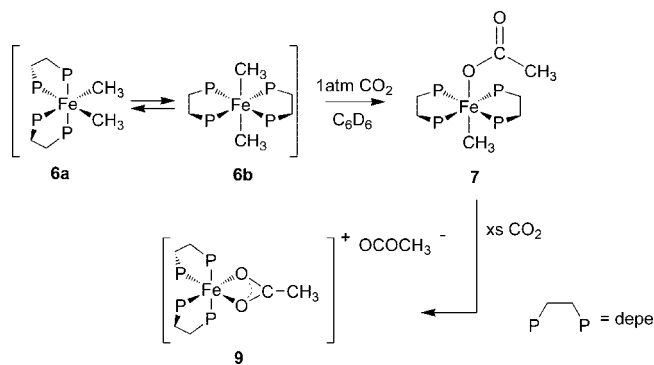


Figure 4. ORTEP diagram of [Fe(depe)₂(η²-O₂CCH₃)]⁺[BPh₄]⁻ (**9**·BPh₄) (50% ellipsoids with hydrogen atoms and counterion omitted for clarity).

Table 4. Selected Bond Distances and Angles for [Fe(depe)₂(η²-O₂CCH₃)]⁺[BPh₄]⁻ (**9**·BPh₄)

Bond Distances (Å)			
Fe(1)–P(1)	2.2881(19)	Fe(1)–P(2)	2.1956(8)
Fe(1)–O(1)	2.0546(8)	O(1)–C(11)	1.857(4)
C(11)–C(12)	1.497(6)		
Bond Angles (deg)			
O(1)–Fe(1)–O(1)	63.52(11)	P(1)–Fe(1)–P(2)	85.52(3)
P(2)–Fe(1)–O(1)	95.78(6)	O(1)–Fe(1)–P(1)	84.68(6)

Scheme 2



Reaction of the depe analogue Fe(depe)₂Me₂ (**6**) with CO₂ yields the expected *trans* monoinsertion product *trans*-Fe(depe)₂(O₂CCH₃)Me (**7**), which exhibits a singlet in the ³¹P{¹H} NMR spectrum at 77.4 ppm and a new pentet at high field in the ¹H spectrum at –3.32 ppm. The reaction is sensitive to heat, and only an insoluble precipitate is produced if the temperature is raised above 298 K. Unlike the dmpe analogue, when higher pressures of CO₂ were employed, the bis-acetate Fe(depe)₂(O₂CCH₃)₂ (**8**) was not observed and the only product observed was the salt [Fe(depe)₂(η²-OCOMe)]⁺[COOMe]⁻ (**9**) (Scheme 2). This is not unreasonable since the bulk of the depe ligands would be expected to favor the single bidentate η²-acetate ligand rather than two η¹-acetates. The ³¹P{¹H} NMR spectrum of **9** exhibits the expected pair of virtual triplets, and the IR spectrum displays bands at 1578 and 1464 cm⁻¹ corresponding to the asymmetric and symmetric stretch of the acetate ligand, respectively.

An alternative route to **9**·BPh₄ is via the addition of sodium acetate to Fe(depe)₂Cl₂ in acetone followed by anion exchange by the addition of sodium tetraphenylborate. Layering of an acetone solution of **9** with pentane produced a crystal suitable

for structure determination by X-ray crystallography (Figure 4). Selected bond lengths and bond angles are listed in Table 4. Complex **9**·BPh₄ exhibits a distorted octahedral geometry with the distortion due mainly to the constraints imposed by the chelating acetate. The angle subtended by the acetate ligand is 63.52(11)°, which is on average 4° larger than the nearest ruthenium analogues, [Ru(dppe)₂(η²-O₂CCH₃)]⁺[PF₆]⁻·2MeOH²⁹ and [Ru(dpmp)₂(η²-O₂CCH₃)]⁺[BPh₄]⁻.³⁰

Formation of Iron Carbonate Complexes. In the reaction of **1** with CO₂, the carbonate complex Fe(dmpe)₂(η²-O₂CO) (**5**) was always formed. This complex has only limited solubility in benzene-*d*₆, so this complex is not seen as a major product in NMR spectra. From the reaction of **1** with CO₂ in C₆D₆, a red crystal of the carbonate complex **5** was grown over a period of 48 h. An ORTEP plot of the structure is given in Figure 5, and details of the core bond angles and bond lengths are given in Table 5.

For complex **5**, the crystallographic asymmetric unit consists of one Fe(dmpe)₂(CO₃) molecule in close association with a H₂CO₃ molecule (Figure 5). There is considerable disorder in the dmpe ligands, and this required the use of multiple sites for most atoms.

The mechanism of formation of the carbonate complex is not clear. The carbonate could be the result of CO₂ disproportionation (effectively to CO₃²⁻ and CO), and metal-catalyzed CO₂ disproportionation has been observed in other metal systems.^{31,32}

The carbonate could also arise from carbonic acid formed from the reaction of CO₂ with adventitious water in the reaction

(29) Lucas, N. T.; Powell, C. E.; Humphrey, M. G. *Acta Crystallogr., Sect. C: Cryst. Struct. Commun.* **2000**, C56, E392–E393.

(30) Boyar, E. B.; Harding, P. A.; Robinson, S. D.; Brock, C. P. *Dalton Trans.* **1986**, 1771–1778.

(31) Alvarez, R.; Atwood, J. L.; Carmona, E.; Perez, P. J.; Poveda, M. L.; Rogers, R. D. *Inorg. Chem.* **1991**, 30, 1493–1499.

(32) Fachinetti, G.; Floriani, C.; Chiesi-Villa, A.; Guastini, C. *J. Am. Chem. Soc.* **1979**, 101, 1767–1775.

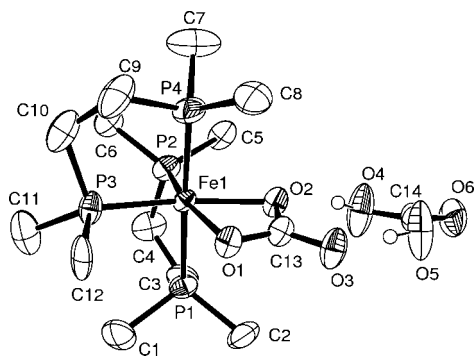
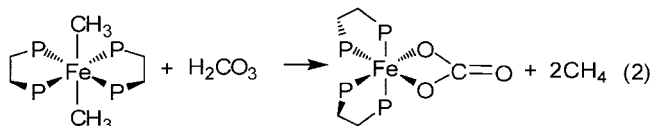
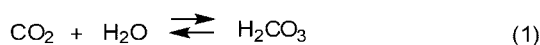


Figure 5. Anisotropic displacement ellipsoid plot of isomer 1 of $[\text{Fe}(\text{dmpe})_2(\text{CO}_3)] \cdot \text{H}_2\text{CO}_3$ (**5**) with labeling of selected atoms. Ellipsoids show 30% probability levels. Hydrogen atoms of the H_2CO_3 are shown as circles of arbitrary radii, and all other H atoms have been deleted for clarity.

Table 5. Selected Bond Distances and Angles for $[\text{Fe}(\text{dmpe})_2(\text{CO}_3)] \cdot \text{H}_2\text{CO}_3$ (**5**)

Bond Distances (Å)			
Fe(1)–P(1)	2.2400(10)	Fe(1)–P(4)	2.2442(10)
Fe(1)–P(2)	2.2195(12)	Fe(1)–P(3)	2.193(4)
Fe(1)–O(1)	2.041(2)	Fe(1)–O(2)	2.039(2)
O(1)–C(13)	1.281(4)	O(2)–C(13)	1.313(4)
O(3)–C(13)	1.262(4)		
Bond Angles (deg)			
P(1)–Fe(1)–P(4)	177.33(4)	P(1)–Fe(1)–P(2)	83.33(7)
P(1)–Fe(1)–P(3)	94.66(9)	P(4)–Fe(1)–P(2)	98.91(7)
P(2)–Fe(1)–P(3)	99.34(12)	P(4)–Fe(1)–P(3)	86.43(9)
O(1)–Fe(1)–O(2)	64.48(9)	O(1)–C(13)–C(2)	114.1(3)
O(2)–C(13)–O(3)	121.7(3)	O(1)–C(13)–O(3)	124.2(3)
Fe(1)–O(1)–C(13)	91.12(18)	Fe(1)–O(2)–C(13)	90.29(19)

Scheme 3



mixture (Scheme 3), and even with scrupulous drying of reagents and solvents it is difficult to completely eliminate this possibility.^{33,34}

Conclusions

Iron dimethyl complexes of the type $\text{Fe}(\text{PP})_2\text{Me}_2$ exist as equilibrating mixtures of *cis*- and *trans*-isomers. Photoisomerization under UV irradiation produces exclusively the *trans*-isomer, but this equilibrates over time to produce an equilibrium mixture of complexes with the *cis* and *trans* stereochemistry. The complex with $\text{PP} = \text{depe}$ is significantly more stereochemically labile than the analogous complex with $\text{PP} = \text{dmpe}$, and this is consistent with the more facile phosphine dissociation for the bulkier *depe* ligand.

The dimethyl complexes react with CO_2 to produce monoacetate and bis-acetate products by insertion of CO_2 sequentially into the two metal–carbon bonds. These reactions probably proceed via a partial dissociation of one of the bidentate phosphine ligands to give a free coordination site for carbon

dioxide binding prior to the migration of the methyl group. The reaction of CO_2 with late metal centers plays an important part in the understanding of the activation of small molecules by transition metals and could lead to systems for the catalytic activation of CO_2 and the incorporation of CO_2 into organic structures as an alternative one-carbon starting material.

Experimental Section

General Information. All manipulations were carried out using standard Schlenk techniques. Air-sensitive NMR samples were prepared in a nitrogen-filled glovebox, with solvent vacuum-transferred into an NMR tube fitted with a concentric Teflon valve. Toluene- d_8 and benzene- d_6 were dried over sodium/benzophenone and vacuum-distilled immediately prior to use. Acetone- d_6 was dried over boric acid and stored over molecular sieves. Methanol- d_4 was dried over molecular sieves. Diethyl ether, hexane, pentane, toluene, and benzene were dried over sodium wire before distillation under nitrogen from sodium/benzophenone. All compressed gases were obtained from the British Oxygen Co. Carbon dioxide (>99.995%) was used as received. ^1H , ^{31}P , and ^{13}C NMR spectra were recorded on a Bruker DRX300 NMR spectrometer at 300.1, 121.5, and 75.5 MHz, respectively, and referenced as follows: ^1H : methyl resonance of toluene- d_8 residual at δ 2.09; benzene- d_6 residual at δ 7.15, THF- d_8 residuals at 3.58 and 1.73, and the methyl resonance of the CD_3OD residual at δ 3.31 ppm. ^{31}P : external phosphoric acid in D_2O at 0.0 ppm. ^{13}C : toluene- d_8 at δ 20.4, benzene- d_6 at δ 128.0, THF- d_8 at δ 67.57 and 25.37, and CD_3OD at δ 49.15 ppm. $\text{Fe}(\text{dmpe})_2\text{Cl}_2$ was prepared following literature methods.²¹

Synthesis of *trans*- $\text{Fe}(\text{dmpe})_2\text{Me}_2$ (1**).** $\text{Fe}(\text{dmpe})_2\text{Cl}_2$ (0.77 g, 1.8 mmol) was dissolved in diethyl ether (50 mL), and a slight excess of methyl lithium (1.5 M in diethyl ether, 3 mL) was added. The color of the reaction mixture changed from green to red immediately and then to orange after 2 h. The solvent was removed *in vacuo*, and the product was extracted into pentane (100 mL). The orange pentane solution was concentrated to 10 mL and cooled to 255 K to produce crystals of *trans*- $\text{Fe}(\text{dmpe})_2\text{Me}_2$ (**1b**) suitable for X-ray crystallographic analysis. If the pentane is removed *in vacuo*, a mixture of the *cis*- and *trans*-**1a** and **1b** isomers was obtained (0.4 g, 58%). NMR spectra were identical to those reported.²¹

Synthesis of *trans*- $\text{Fe}(\text{dmpe})_2(\text{O}_2\text{CCH}_3)\text{Me}$ (2b**).** NMR Scale. CO_2 (1 atm) was added to a NMR tube containing a degassed solution of $\text{Fe}(\text{dmpe})_2\text{Me}_2$ (**1**) (0.02 g, 0.05 mmol) in C_6D_6 . The NMR tube was then allowed to warm to room temperature, and after 1 h, the NMR spectrum showed peaks attributable to **2**.

Preparative Scale. A solution of acetic acid (0.5 M, 2.26 mL, 1.1 mmol) was added dropwise to a solution of *trans*- $\text{Fe}(\text{dmpe})_2(\text{CH}_3)_2$ (**1**) (0.44 g, 1.1 mmol) in diethyl ether (75 mL) at -80°C . After 5 min the color of the mixture had changed to dark red, the mixture was allowed to warm to room temperature and stirred for a further 18 h. The solvent was removed *in vacuo* to leave a dark red solid, which was washed in cold pentane to remove residual starting material. The desired product was recrystallized from hexane at -20°C . *trans*- $\text{Fe}(\text{dmpe})_2(\text{O}_2\text{CCH}_3)\text{Me}$ (**2b**) was obtained as a dark red solid (0.1 g, 0.2 mmol, 21%). Anal. Calcd for $\text{C}_{15}\text{H}_{38}\text{FeO}_2\text{P}_4$. C, 41.88; H, 8.90. Found: C, 41.99; H, 9.00. $^{31}\text{P}\{^1\text{H}\}$ NMR (C_6D_6 , 121.5 MHz, 298 K): δ 71.1 (s) ppm. ^1H NMR (C_6D_6 , 300 MHz, 298 K): δ -3.29 (p, 3H, FeCH_3), 1.01 (s, 12H, PCH_3), 1.29 (s, 12H, PCH_3), 1.39–1.57 (m, 4H, PCH_2), 1.73 (s, 3H FeO_2CCH_3), 2.03–2.15 (m, 4H, PCH_2) ppm. Selected $^{13}\text{C}\{^1\text{H}\}$ NMR (C_6D_6 , 75 MHz, 298 K): δ -33.4 (FeCH_3), 24.4 (FeO_2CCH_3) 176.2 (FeO_2CCH_3) ppm. IR (Fluorolube): 1600 ($\nu_{\text{asym}}(\text{CO}_2)$), 1322 ($\nu_{\text{sym}}(\text{CO}_2)$) cm^{-1} .

Formation of *cis*- $\text{Fe}(\text{dmpe})_2(\text{O}_2\text{CCH}_3)\text{Me}$ (2a**).** An NMR tube containing a sample of *trans*- $\text{Fe}(\text{dmpe})_2(\text{O}_2\text{CCH}_3)\text{Me}$ (**2b**) in C_6D_6 was irradiated with a 300 W mercury vapor lamp for 18 h, during

(33) Pushkar, J.; Wendt, O. F. *Inorg. Chim. Acta* **2004**, *357*, 1295–1298.

(34) Crutchley, R. J.; Powell, J.; Faggiani, R.; Lock, C. J. L. *Inorg. Chim. Acta* **1977**, *24*, L15–L16.

Table 6. Crystal Data and Refinement Details for 1b, 3, 5, 6b, and 9

	1b	3	5	6b	9
empirical formula	C ₁₄ H ₃₈ P ₄ Fe ₁	C ₁₆ H ₃₈ P ₄ O ₄ Fe	C ₁₃ H ₃₂ P ₄ O ₃ Fe·CH ₂ O ₃	C ₂₂ H ₅₄ P ₄ Fe	C ₄₆ H ₇₁ P ₄ O ₂ BFe
<i>M</i>	193.09	474.19	478.17	498.38	846.57
temp (K)	173(2)	150(2)	200(2)	223(2)	223(2)
cryst syst	monoclinic	tetragonal	orthorhombic	triclinic	orthorhombic
space group	<i>P</i> 2 ₁ / <i>c</i>	<i>P</i> 4 ₁ 2 ₁ 2	<i>Pbca</i>	<i>P</i> $\bar{1}$	<i>Ibca</i>
unit cell dimens					
<i>a</i> (Å)	8.762(2)	8.990(1)	16.5175(3)	7.5930(4)	17.3563(4)
<i>b</i> (Å)	12.581(3)	8.990(1)	16.1088(3)	10.2012(4)	22.1987(6)
<i>c</i> (Å)	12.814(2)	28.589(3)	16.66269(3)	19.5659(10)	24.0438(6)
α (deg)				77.903(2)	
β (deg)	132.979(9)			89.807(2)	
γ (deg)				68.634(4)	
<i>V</i> (Å ³)	1033.4(4)	2310.6(4)	4424.04(14)	1375.59(11)	9263.8(4)
<i>Z</i>	2	4	8	2	8
ρ (calc) (g cm ⁻³)	1.241	1.363	1.436	1.203	1.214
μ (Mo K α) (mm ⁻¹)	1.029	0.947	0.7107	0.788	0.499
<i>N</i>	6363	23152	57391	17578	88581
<i>N</i> _{ind}	2269	2829	5078	4530	5357
<i>N</i> _{obs} (<i>I</i> > 2 σ (<i>I</i>))	1998	2749	5060	4004	4144
R1(<i>F</i>) ^a	0.0531	0.0174	0.0384	0.0565	0.0567
wR2(<i>F</i> ²)	0.1361	0.0488	0.1174	0.1069	0.1545

^a R1 = $\sum ||F_o| - |F_c|| / \sum |F_o|$ for $F_o > 2\sigma(F_o)$; wR2 = $(\sum w(F_o^2 - F_c^2)^2 / \sum w(F_c^2)^2)^{1/2}$ all reflections $w = 1/[\sigma^2(F_o^2) + (0.04P)^2 + 5.0P]$ where $P = (F_o^2 + 2F_c^2)/3$.

which time peaks attributable to **2a** and **2b** were distinct in the NMR spectra. *cis*-Fe(dmpe)₂(O₂CCH₃)Me (**2a**) ³¹P{¹H} NMR (C₆D₆, 121.5 MHz, 298 K): δ 55.8 (m, phosphorus *trans* to methyl group), 59.5 (m, phosphorus *trans* to phosphorus), 70.2 (ddd, *J*_{PP} = 18.7 Hz, *J*_{PP} = 49.7 Hz, *J*_{PP} = 166.9 Hz), 75.0 (m, phosphorus *trans* to acetate group) ppm. ¹H NMR (C₆D₆, 300 MHz, 298 K): δ 0.07 (m, 3H FeCH₃), 0.39 (d, 3H, 1 \times PCH₃, *J*_{PH} = 9.9 Hz), 0.59 (d, 3H, 1 \times PCH₃, *J*_{PH} = 9.9 Hz), 0.92 (d, 3H, 1 \times PCH₃, *J*_{PH} = 10.8 Hz), 0.98 (d, 3H, 1 \times PCH₃, *J*_{PH} = 9.5 Hz), 1.03 (bs, 1 \times PCH₃), 1.09 (d, 3H, 1 \times PCH₃, *J*_{PH} = 11.9 Hz), 1.24–1.35 (br m, 2H, PCH₂), 1.25 (bs, 3H, PCH₃), 1.37 (d, 3H, 1 \times PCH₃, *J*_{PH} = 11.4 Hz), 1.38 (br m, 2H, PCH₂), 1.49 (br m, 2H, PCH₂), 1.74 (br m, 2H, PCH₂), 2.02 (bs, 3H, OCH₃) ppm. Selected ¹³C{¹H} (C₆D₆, 75 MHz, 298 K): δ -3.9 (FeCH₃), 25.4 (FeO₂CCH₃) 175.9 (FeO₂CCH₃) ppm.

Synthesis of *trans*-Fe(dmpe)₂(O₂CCH₃)₂ (3). NMR Scale. CO₂ (3–4 atm) was condensed into a NMR tube frozen in liquid N₂ containing a degassed solution of Fe(dmpe)₂Me₂ (**1**) (0.02 g, 0.05 mmol) in C₆D₆. The NMR tube was then allowed to warm to room temperature, and after 2 days the NMR spectrum showed **3** to be the main product.

Preparative Scale. Dmpe (1.33 g, 8.8 mmol) as a solution in THF (50 mL) was added to a slurry of Fe(CH₃CO₂)₂ (0.77 g, 4.4 mmol) in THF (100 mL). After 2 h, a blue powder had precipitated. The residue was isolated by filtration and dried *in vacuo*. Crystals suitable for X-ray analysis were obtained by layering a DMF solution with pentane (0.63 g, 1.3 mmol, 30%). Anal. Calcd for C₁₆H₃₈FeO₄P₄: C, 40.52; H, 8.08. Found: C, 40.60; H, 7.94. ³¹P{¹H} NMR (toluene-*d*₈, 121.5 MHz, 300 K): δ 64.5 (s) ppm. ¹H NMR (toluene-*d*₈, 300 MHz, 300 K): δ 1.20 (s, 24H, PCH₂), 1.22 (s, 6H, FeO₂CCH₃), 2.39 (bs, 8H, PCH₂) ppm. ¹³C{¹H} NMR (toluene-*d*₈, 75 MHz, 300 K): δ 14.0 (m, 8C, PCH₃), 23.6 (s, FeO₂CCH₃), 30.3 (m, PCH₂), 177.3 (s, FeO₂CCH₃) ppm. IR (Fluorolube): 1606 ($\nu_{\text{asym}}(\text{CO}_2)$), 1323 ($\nu_{\text{sym}}(\text{CO}_2)$) cm⁻¹.

Synthesis of {*cis*-Fe(dmpe)₂(η^2 -O₂CCH₃)₂}⁺{O₂CCH₃}⁻ (4). *trans*-Fe(dmpe)₂(O₂CCH₃)₂ (**3**) (0.02 g) was dissolved in CD₃OD (0.5 mL). The solution immediately turned a deep red color indicating the formation of **4**. ³¹P{¹H} NMR (CD₃OD, 121.5 MHz, 298 K): δ 63.5 (apparent triplet, splitting = 41.3 Hz), 72.9 (apparent triplet, splitting = 41.3 Hz). ³¹P{¹H} NMR (CD₃OD, 300 MHz, 298 K): δ 1.10 (s, 6H 2 \times PCH₃), 1.13 (s, 6H, 2 \times PCH₃), 1.46 (s, 6H, 2 \times PCH₃), 1.68 (s, 3H, 1 \times CH₃COO), 1.79 (s, 6H, 2 \times PCH₃), 1.87 (s, 1 \times CH₃COO), 2.11 (m, 4H, 1 \times PCH₂), 2.21 (m, 4H, 1 \times PCH₂) ppm. ¹³C{¹H} (CD₃OD, 75 MHz, 298 K): δ 10.8

(m, PCH₃), 13.2 (m, PCH₃), 16.3 (m, PCH₃), 17.2 (m, PCH₃), 24.3 (s, CH₃COO), 24.4 (s, CH₃COO), 27.6 (m, PCH₂), 29.0 (m, PCH₂), 179.7 (O₂CCH₃), 184.5 (O₂CCH₃) ppm.

Synthesis of *cis*-Fe(CO)₃(dmpe)₂ (5). Fe(dmpe)₂Cl₂ (0.27 g, 0.63 mmol) was dissolved in methanol (50 mL), and an excess of K₂CO₃ was added, affording a bright orange-red solution immediately. The mixture was stirred for 2 h, and the solvent was removed *in vacuo* to leave a red powder (0.2g, 80%). ³¹P{¹H} NMR (CD₃OD, 121.5 MHz, 300 K): δ 65.7 (2P, apparent triplet, splitting = 38.3 Hz), 74.7 (2P, apparent triplet, splitting = 38.3 Hz) ppm. ¹H NMR (CD₃OD, 300 MHz, 300 K): δ 1.34, 1.39, 1.60, 1.83 (24H, 4 \times d, 4 PCH₃), 2.15–2.35 (8H, 2 \times m, 4CH₂) ppm. Selected ¹³C{¹H,³¹P} NMR (CD₃OD, 75 MHz, 300 K): δ 9.7, 14.8, 16.3, 17.9 (4 \times s, 4 P(CH₃)₂), 27.7, 33.9 (2 \times s, 4CH₂ 166.5 (s, CO₃) ppm. MS [ESI; *m/z*, (%)] 417.0, (50).

Synthesis of *trans*-Fe(depe)₂Me₂ (6). Fe(depe)₂Cl₂ (1.64 g, 3 mmol) was dissolved in diethyl ether (75 mL), and a slight excess of methyllithium (1.5 M in diethyl ether, 5 mL) was added. The color of the reaction mixture changed from green to red immediately and eventually to orange after 2 h. The solvent was removed *in vacuo* and the product extracted into pentane (100 mL). The orange pentane solution was concentrated to 10 mL and cooled to 255 K to produce crystals of *trans*-Fe(depe)₂Me₂ (**6b**) suitable for X-ray crystallographic analysis. If the pentane was removed *in vacuo*, a mixture of the *cis*- and *trans*-isomers (**6a** and **6b**) was obtained (0.63 g, 42%). Anal. Calcd for C₂₂H₅₄FeP₄: C, 53.02; H, 10.92. Found: C, 52.73; H, 11.08. *cis*-Fe(depe)₂Me₂ (**6a**): ³¹P{¹H} NMR (C₆D₆, 121.5 MHz, 300 K): δ 60.7 (apparent triplet, splitting = 23 Hz), 81.6 (apparent triplet, splitting = 23 Hz) ppm. Selected ¹H NMR (C₆D₆, 300 MHz, 300 K): δ -0.55 (multiplet, FeCH₃) ppm. Selected ¹³C{¹H} (C₆D₆, 75 MHz, 300 K): δ -3.28 (1C, FeCH₃) ppm. *trans*-Fe(depe)₂Me₂(CH₃)₂ (**6b**): ³¹P{¹H} NMR (C₆D₆, 121.5 MHz, 300 K): δ 84.3 (s) ppm. Selected ¹H NMR (C₆D₆, 300 MHz, 300 K): δ -2.00 (p, ³*J*_{PH} = 5.7 Hz, FeCH₃) ppm. Selected ¹³C{¹H} (C₆D₆, 75 MHz, 300 K): δ -22.2 (FeCH₃) ppm. MS [ESI (NH₃); *m/z* (%)] 498 (0.1%) M⁺.

Synthesis of *trans*-Fe(depe)₂(O₂CCH₃)(CH₃) (7). NMR Scale. CO₂ (1 atm) was added to a NMR tube containing a degassed solution of Fe(depe)₂Me₂ (**6**) (0.023 g, 0.05 mmol) in C₆D₆ at room temperature. The NMR tube was allowed to warm to room temperature, and after 30 min the NMR spectrum displayed resonances attributable to **7**.

³¹P{¹H} NMR (C₆D₆) (121.5 MHz, 300 K): δ 77.4 (s) ppm. Selected ¹H NMR (C₆D₆, 300 MHz, 300 K): δ -3.32 (p, 3H, FeCH₃)

ppm. Selected $^{13}\text{C}\{^1\text{H}\}$ (C_6D_6 , 75 MHz, 300 K): δ 177.3 (s, FeO_2CCH_3) ppm.

Synthesis of $\{\text{cis-Fe}(\text{depe})_2(\eta^2\text{-O}_2\text{CCH}_3)\}^+\{\text{BPh}_4\}^- (\mathbf{8} \cdot \text{BPh}_4)$. Two equivalents of sodium acetate (0.12 g, 1.4 mmol) were added to a slurry of *cis*- $\text{Fe}(\text{depe})_2\text{Cl}_2$ (0.4 g, 0.7 mmol) in acetone. Over the space of a few minutes, the color of the solution changed from green to dark red. The mixture was left to stir for 1 h before 1 equiv of NaBPh_4 (0.24 g, 0.7 mmol) was added. The color of the mixture darkened, and it was left to stir for 18 h. The mixture was filtered via a canula and layered with pentane to give large purple crystals, which were suitable for X-ray analysis (0.42 g, 0.5 mmol, 71%). Anal. Calcd for $\text{C}_{46}\text{H}_{72}\text{FeBO}_2\text{P}_4$: C, 65.26; H, 8.45. Found: C, 64.94; H, 8.49. $^{31}\text{P}\{^1\text{H}\}$ NMR (acetone- d_6 , 121.5 MHz, 300 K): δ 80.6 (apparent triplet, splitting = 40 H), 71.8 (apparent triplet, splitting = 40 H) ppm. ^1H NMR (acetone- d_6 , 300 MHz, 300 K): δ 7.31 (m, 8H, *ortho H* of $\text{C}_6\text{H}_5\text{B}$), 6.92 (m, 8H, *meta H* of $\text{C}_6\text{H}_5\text{B}$), 6.77 (m, 4H, *para H* of $\text{C}_6\text{H}_5\text{B}$), 1.91–2.27 (m, 24H, PCH_2), 1.65

(s, 3H, FeO_2CCH_3), 1.18, 1.08 (2 \times m, 24H, CH_2CH_3) ppm. $^{13}\text{C}\{^1\text{H}, ^{31}\text{P}\}$ NMR (acetone- d_6 , 300 MHz, 300 K): δ 183.7 (s, FeO_2CCH_3), 165.2 (s, quaternary B(C_6H_5) $_4$), 136.9, 125.8, 122.0 (3s, B(C_6H_5) $_4$), 24.4 (s, FeO_2CCH_3), 23.6, 23.1, 21.4, 19.9, 18.1, 13.0 (PCH_2), 9.3, 8.4, 8.0, 7.3 (PCH_2CH_3) ppm. HRMS [ESI; m/z (%]): 527.220161(7); calcd for $\text{C}_{46}\text{H}_{72}\text{FeBO}_2\text{P}_4$, 527.21937. IR (Fluorolube): 1578 ($\nu_{\text{asym}}(\text{CO}_2)$), 1464 ($\nu_{\text{sym}}(\text{CO}_2)$) cm^{-1} .

Acknowledgment. The authors thank the Australian Research Council for financial support.

Supporting Information Available: A CIF file giving crystallographic data. This material is available free of charge via the Internet at <http://pubs.acs.org>.

OM800091A